Dalton Transactions

Accepted Manuscript

ROYAL SOCIETY OF CHEMISTRY

www.rsc.org/dalton

Dalton Transactions

RSCPublishing

ARTICLE

A Step Closer to the Binary: The $^{1}_{\infty}[Bi_6I_{20}]^{2-}$ Anion

Cite this: DOI: 10.1039/xoxxoooooox

Johanna Heine[a]

Received ooth January 2012,
Accepted ooth January 2012

DOI: 10.1039/xoxxoooooox

www.rsc.org/

A series of crown ether based iodidobismuthates was prepared from dibenzo-18-crown-6 (DB18C6), BiI_3 and NaI or KI in acetonitrile (MeCN). The resulting compounds $[(DB18C6)Na(MeCN)_2]_4[Bi_6I_{22}]\cdot 2MeCN$ (**1**), $[(DB18C6)Na(MeCN)_2]_4[Bi_8I_{28}]\cdot 6MeCN$ (**2**), $[(DB18C6)Na(MeCN)_2]_2[Bi_6I_{20}]\cdot 3MeCN$ (**3**) and $[(DB18C6)K(MeCN)]_4[Bi_6I_{22}]\cdot 2MeCN$ (**4**) have been used to explore the templating effect of different crown ether based cations and the influence of the I/Bi ratio and I…I interactions on the optical properties of iodidobismuthates. Compound **3** contains the strand-like anion $^{1}_{\infty}[Bi_6I_{20}]^{2-}$, which displays a I/Bi ratio of 3.33, closer to the binary BiI_3 than any other iodidobismuthate.

Introduction

Hybrid iodidometalate materials based on transition or main group metals are known for properties such as semiconductivity[1], photoluminescence[2] or ferroelectricity[3]. This is often combined with facile processing at room temperature.[4] As a result, iodidometalate based materials have already been tested for optoelectronic devices[5] such as LEDs (light-emitting diodes)[6], FETs (field-effect transistors)[7] or TFTs (thin-film transistors)[8].

Iodidostannates and plumbates, in the form of hybrid perovskites[9], have recently had a renaissance as a light harvesting component of solar cells[10], generating intense research interest. In contrast, hybrid iodidometalates based on group 15 metals have received less attention.[11]

One reason for this is the preference of iodidobismuthates and their homologues to form a limited number of different molecular cluster anions. Similarly to halogenidocuprates, control over the resulting anionic substructure of iodidobismuthates often remains very difficult.[12] One-dimensional iodidobismuthate anions are rare[13] and only one example has been reported of a two-dimensional iodidobismuthate[14]. This is opposed to iodidostannates and plumbates, where a number of two and three dimensional anions are known besides the prototypical and highly versatile perovskite structure.[11]

Aside from the dimensionality of the anions, iodidometalates can also be classified by their aggregation densities. A simple way to describe these densities, the I/M ratio, has been proposed by *Mercier* and coworkers.[11] For the iodidobismuthates, these lie between 3.00, i.e. the ratio found at binary bismuthiodide BiI_3, and 6.00 for the mononuclear $[BiI_6]^{3-}$ anion.

Despite the seemingly more limited chemistry of iodidobismuthates in contrast to iodidostannates and plumbates, this chemistry might still hold great potential for semiconductor materials for solar applications that are comprised of less toxic elements. In contrast to lead and tin, bismuth compounds are generally considered to be more benign[15] especially in the form of the structurally rich oxo clusters[16] or as a new generation of heterogeneous photocatalysts based on oxyhalide materials.[17]

To gain access to a library of new hybrid iodidobismuthate in a rational manner, the reaction regime outlined in Scheme 1 has been employed. Combining alkali metal iodides with different crown ethers and bismuth iodide and controlling additional parameters such as reagent ratio, solvent and reaction temperature and time leads to a reaction system from which a host of new materials can be generated. The advantages of this system are the ease of crystallization due to the use of crown ethers and the possibility of controlling the cation size and interactions through variation of both the crown ether and the alkali metal cation.

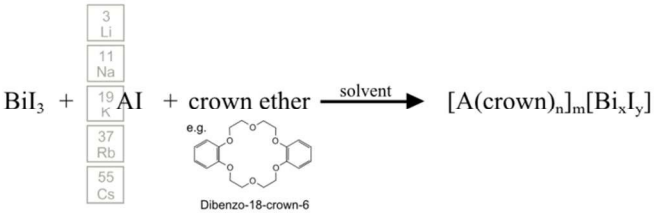

Scheme 1. Reaction system comprised of BiI_3, an alkali metal iodide AI and a crown ether, resulting in a library of new hybrid iodidobismuthate compounds.

Here, one series of compounds obtained from this approach is presented: Iodidobismuthates with $[(DB18C6)A(MeCN)_n]^+$ (DB18C6 = dibenzo-18-crown-6, A = Na, K, n = 1, 2) counterions that cover a range of aggregation densities and thus allow a direct observation structure-property relationships linked to this parameter. The series consists of three sodium compounds, $[(DB18C6)Na(MeCN)_2]_4[Bi_6I_{22}]\cdot 2MeCN$ (**1**; I/Bi 3.67), $[(DB18C6)Na(MeCN)_2]_4[Bi_8I_{28}]\cdot 6MeCN$ (**2**; I/Bi 3.50) and $[(DB18C6)Na(MeCN)_2]_2\,^{1}_{\infty}[Bi_6I_{20}]\cdot 3MeCN$ (**3**; I/Bi 3.33), and the potassium compound $[(DB18C6)K(MeCN)]_4[Bi_6I_{22}]\cdot 2MeCN$ (**4**; I/Bi 3.67). While compounds **1**, **2** and **4** contain iodidobismuthate anions that have been previously reported, the anion found in **3** is unprecedented and possesses an I/Bi ratio of 3.33, closer to the

3.00 of binary BiI_3 than any other known iodidobismuthate anion. The respective anion structures are shown in Scheme 2. Investigations of the optoelectronic properties within the series **1 - 3** reveal a continuous decrease in the optical bandgaps in correlation with the I/Bi ratio. Compounds **1** and **4** each contain hexanuclear iodidobismuthate anions that are arranged in different fashions within the respective crystal structures. This allows for an estimate of how secondary interactions such as I…I contacts, cation shape and conformation can subtly influence properties such as stabilities and bandgaps, a point of on-going examination and discussion in the literature.[13, 18]

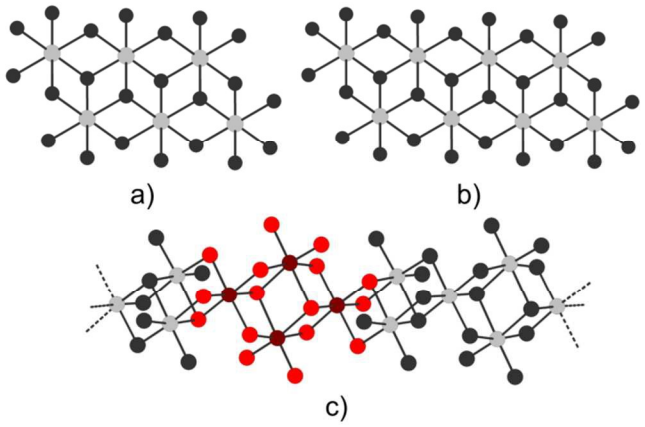

Scheme 2. Schematic representation of the iodidobismuthate anions found in compounds **1-4** with Bi depicted in ligth grey and I depicted in dark grey: a) hexanuclear $[Bi_6I_{22}]^{4-}$ found in **1** and **4**, b) octanuclear $[Bi_8I_{28}]^{4-}$ found in **2** and c) polymeric, chain-like $^1_\infty[Bi_6I_{20}]^{2-}$ shown with two repeating units and one $[Bi_4I_{16}]$ building block highlighted in red for clarity.

Experimental Section

General

BiI_3[19] was sublimed for purification, ground to a fine powder and stored under Argon until used to avoid hydrolysis. Solvents acetonitrile (MeCN) and ethanol (EtOH) were of HPLC-grade, NaI, KI and dibenzo-18-crown-6 were used as received from commercial sources.

Bulk analyses

The CHN analysis was carried out on an *Elementar* CHN-analyzer. A partial loss of solvate acetonitrile can be observed for all compounds. In all cases, the percentages obtained for nitrogen were used to determine the remaining acetonitrile in the dried compounds.

The thermal investigation was carried out by simultaneous DTA/TG on a *NETZSCH STA 409 C/CD* in the temperature range of 25 °C to 800 °C with a heating rate of 10 °C min^{-1} in a constant flow of 80 ml min^{-1} Ar. Freshly isolated material was used for these investigations to determine the amount of solvate acetonitrile lost directly upon isolation from the mother liquor.

Optical absorption spectra were recorded on a *Varian Cary 5000* UV/Vis/NIR spectrometer in the range of 800-200 nm in diffuse reflectance mode employing a Praying Mantis accessory (Harrick). To assure that measurements were performed on the solvated compounds, single crystals of **1-4** were taken fresh from the mother liquor, freed from any adhering liquid on a filter paper, gently crushed into a powder between the filter paper and rapidly brought into the UV-VIS beam. Measurements on were also performed on the same samples after desolvation by drying at 170°C under vacuum for 1 h.

Powder diffraction patterns of **1-4** were recorded on a *Panalytical X'Pert Pro PW3040/60* with $CuK_{\alpha1}$ radiation with $\lambda = 1.54056$ Å or on a *Panalytical X'Pert Pro* with CuK_α radiation with $\lambda = 1.54$ Å and are included in the ESI in Figure S13-S16.

IR spectra of **1-4** were recorded on a *Bruker Tensor 37* FT-IR spectrometer equipped with an ATR-Platinum measuring unit. The spectra are shown in Figure S17-S20 in the ESI.

X-ray crystallography

Single crystal X-ray determination was performed on a on a *STOE IPDS2* diffractometer equipped with an imaging plate detector system using MoKα radiation with graphite monochromatization for compounds **1**, **2** and **4** and on a *Bruker Quest D8* diffractometer with microfocus MoKα radiation and a Photon 100 (CMOS) detector for compound **3**.

The structures were solved using direct methods, refined by full-matrix least-squares techniques and expanded using Fourier techniques, using the Shelx software package[20] within the OLEX2 suite[21]. All non-hydrogen atoms were refined anisotropically, unless indicated otherwise. Hydrogen atoms were assigned to idealized geometric positions and included in structure factors calculations. Pictures of the crystal structures were created using DIAMOND[22]. Generally, despite fast and careful handling of the crystals during the set-up of the measurement, the crystal structures of all four compounds suffer in quality due to loss of solvate acetonitrile to varying degrees, reflected in a number of corresponding B and C level alerts in the checkcif reports.

In the crystal structure refinement of **2**, one carbon atom had to be restrained with an ISOR command to allow for a reasonable anisotropic refinement. Crystals of compound **3** suffer severely from rapid degradation upon solvent loss. Despite many tries and attempts to measure at different temperatures, only samples displaying crystal splitting could be mounted for measurement. Thus, the dataset had to be refined as a two-component non-merohedral twin. To correctly model the $[(DB18C6)Na(MeCN)_2]^+$ cations, a number of ISOR restraints had to be employed. Non-coordinating solvent molecules were refined isotropically. In the refinement of **4**, a number of anti-bumping restraints had to be used to ensure reasonable distances between potassium and carbon atoms. Additionally, a number of SIMU restraints were used to obtain reasonable anisotropic displacement parameters for the carbon atoms within the crown ether moiety.

Crystal data and structure refinement details for **1-4** have been summarized in Table 2 and selected bond length and bond angles shown in Tables S1-S4 in the ESI. The data for **1-4** has also been deposited as CCDC 1050429-1050432.

Dalton Transactions RSCPublishing

ARTICLE

Table 2. Crystallographic data of **1**-**4**.

	1	**2**	**3**	**4**
Empirical formula	$C_{100}H_{126}Bi_6I_{22}N_{10}Na_4O_{24}$	$C_{108}H_{138}Bi_8I_{28}N_{14}Na_4O_{24}$	$C_{54}H_{69}Bi_6I_{20}N_7Na_2O_{12}$	$C_{46}H_{57}Bi_3I_{11}K_2N_3O_{12}$
Formula weight /g·mol^{-1}	5989.74	7333.32	4846.02	2944.98
Crystal color and shape	orange block	red plate	red block	red block
Crystal size	0.51 x 0.20 x 0.18	0.18 x 0.08 x 0.004	0.151 x 0.145 x 0.132	0.36x0.26x0.20
Crystal system	triclinic	triclinic	triclinic	monoclinic
Space group	*P*-1	*P*-1	*P*-1	$P2_1/n$
a /Å	14.0239(7)	13.7807(6)	14.372(3)	19.4954(11)
b /Å	14.4683(7)	14.9735(7)	19.388(3)	16.2145(6)
c /Å	21.9043(15)	23.0161(9)	19.648(4)	23.3300(13)
α /°	100.800(6)	85.620(3)	96.034(5)	90
β /°	101.549(6)	88.702(3)	100.883(5)	92.905(5)
γ /°	109.797(4)	74.572(3)	102.490(5)	90
V /Å^3	3937.0(4)	4564.7(3)	5187.9(16)	7365.3(6)
Z	1	1	2	4
ρ_{calc} /g·cm^{-3}	2.526	2.668	3.102	2.656
$\mu(Mo_{K\alpha})$ /mm^{-1}	11.063	12.480	16.146	11.923
measurement temp. /K	100	100	100	100
Absorption correction type	multi-scan	multi-scan	multi-scan	multi-scan
Min/max transmission	0.0582/0.0119	0.4112/ 0.1531	0.394403/0.745196	0.0857/0.5364
2*Θ* range /°	3.11-53.61	2.83-53.58	4.64-50.87	2.656-53.706
No. of measured reflections	46310	49426	103600	79147
No. of independent reflections	16638	19279	18828	15628
R(int)	0.1308	0.1285	0.0566	0.2233
No. of indep. reflections ($I > 2\sigma(I)$)	9547	9545	15244	9570
No. of parameters	753	845	873	697
R_1 ($I > 2\sigma(I)$)	0.0469	0.0594	0.0576	0.0666
wR_2 (all data)	0.1013	0.1390	0.1205	0.1618
S (all data)	0.858	0.831	1.116	0.928
$\Delta\rho_{max}$, $\Delta\rho_{min}$ /e· Å^{-3}	2.202/-3.315	3.118/-4.478	3.734/-1.763	3.126/-2.195

Syntheses and combustion analysis data

Synthesis of [(DB18C6)Na(MeCN)$_2$]$_4$[Bi$_6$I$_{22}$]·2MeCN (**1**). A mixture of NaI (15 mg, 0.1 mmol), DB18C6 (36 mg, 0.1 mmol) and BiI_3 (74 mg, 0.12 mmol) was suspended in 10 mL MeCN and heated at reflux for one hour. A minimum amount of black solid was removed from the resulting deep red solution via filtration. The solution was stored at 4°C. After one day, orange rod-like crystals could be observed in the solution. After one week, the crystals were isolated via filtration and washed with 10 mL of EtOH to remove the mother liquor, dried in air for a few minutes on the filter paper and stored under Argon. The yield was 47 mg (40 % with respect to BiI_3).

Data for **1**: Anal. Calcd for $Na_4Bi_6I_{22}C_{87.4}H_{107.1}O_{24}N_{3.7}$, (M = 5731.2357 g mol^{-1}): C, 18.32; H, 1.88; N, 0.90%. Found: C, 17.94; H, 1.841; N, 0.90%.

Synthesis of $[(DB18C6)Na(MeCN)_2]_4[Bi_8I_{28}]\cdot 6MeCN$ (2). A mixture of NaI (15 mg, 0.1 mmol), DB18C6 (36 mg, 0.1 mmol) and BiI_3 (83 mg, 0.14 mmol) was suspended in 15 mL MeCN and heated at reflux for one hour. A minimum amount of orange solid was removed from the resulting deep red solution via filtration. The solution was stored at 4°C. After three days red sheet-like crystals could be observed in the solution. After one week, the crystals were isolated via filtration and washed with 5 mL of EtOH to remove the mother liquor, dried in air for a few minutes on the filter paper and stored under Argon. The yield was 34 mg (20 % with respect to BiI_3).

Data for **2**: Anal. Calcd for $Na_4Bi_8I_{28}C_{100}H_{126}O_{24}N_{10}$, (M = 7169.2505 g mol^{-1}): C, 16.75; H, 1.77; N, 1.95%. Found: C, 16.31; H, 1.691; N, 1.93 %.

Synthesis of $[(DB18C6)Na(MeCN)_2]_2[Bi_6I_{20}]\cdot 3MeCN$ (3). A mixture of NaI (15 mg, 0.1 mmol), DB18C6 (36 mg, 0.1 mmol) and BiI_3 (177 mg, 0.3 mmol) was suspended in 40 mL MeCN and heated at reflux for one hour. A black solid was removed from the resulting deep red solution via filtration. The solution was stored at 4°C. After one day, dark red needle-like crystals could be observed in the solution. After one week, the crystals were isolated via filtration and washed with 5 mL of EtOH to remove the mother liquor, dried in air for a few minutes on the filter paper and stored under Argon. The yield was 75 mg (30 % with respect to BiI_3).

Data for **3**: Anal. Calcd for $Na_2Bi_6I_{20}C_{46.4}H_{58.6}O_{12}N_{3.2}$, (M = 4691.1273 g mol^{-1}): C, 11.88; H, 1.26; N, 0.96%. Found: C, 11.35; H, 1.146; N, 0.96%.

Synthesis of $[(DB18C6)K(MeCN)]_4[Bi_6I_{22}]\cdot 2MeCN$ (4). A mixture of KI (16 mg, 0.1 mmol), DB18C6 (36 mg, 0.1 mmol) and BiI_3 (117 mg, 0.2 mmol) was suspended in 10 mL MeCN and heated at reflux for one hour. Red and black solids were removed from the resulting deep red solution via filtration. The solution was stored at room temperature. Within one hour, red, block-shaped crystals could be observed in the solution. After one day, the crystals were isolated via filtration and washed with 5 mL of EtOH to remove the mother liquor, dried in air for a few minutes on the filter paper and stored under Argon. The yield was 85 mg (60 % with respect to KI/DB18C6).

Data for **4**: Anal. Calcd for $K_4Bi_6I_{22}C_{85.8}H_{104.7}O_{24}N_{2.9}$, (M = 5762.8284 g mol^{-1}): C, 17.88; H, 1.83; N, 0.70%. Found: C, 17.61; H, 1.788; N, 0.69%.

Results and discussion

Synthesis

Compounds **1-3** have been obtained from acetonitrile solutions containing the starting materials NaI, DB18C6 and BiI_3 in different ratios. They show a significant tendency to co-crystallize from the same reaction solutions. Thus, the synthesis of each compound had to be optimized to yield crystals of only one species. As a result, reactions leading to **1** and **2** are performed with sub-stoichiometric amounts of BiI_3. Additionally, the solubility of the compounds decreases from **1** to **3** and thus a continuously larger amount of solvent had to be used in the respective reactions to ensure an adequate crystallization rate.

The observed co-crystallization of **1-3** points towards a complex equilibrium of $[Bi_nI_m]^{q-}$ species in solution that is governed not only by the reagent ratio, but also by the crystallization tendency of the compounds containing each species of anion, a phenomenon that has been noted before in a larger context as well. [11]

Compound **4** can be obtained in the same manner as compounds **1-3** when employing KI instead of NaI. Interestingly, **4** appears to be the favored species, crystallizing from solutions with reagent ratios ranging from 1:1:2 to 1:1:3 for KI:DB18C6:BiI_3 with no additional phases in evidence.

Description of the crystal structures

Compound **1** crystallizes in the triclinic space group *P*-1. The asymmetric unit contains one half of a $[Bi_6I_{22}]^{4-}$ anion, two $[(DB18C6)Na(MeCN)_2]^+$ cations and two MeCN solvent molecules. Each $[Bi_6I_{22}]^{4-}$ anion consists of six edge-sharing BiI_6 octahedra. These octahedra are arranged in a planar sheet that represents a cutout of a single layer of PbI_2, as shown in Scheme 2. Such hexanuclear anions have been reported for several heavier group 15 halogenidometalates[23] and appear to represent one of the more favored structural motifs. Bi-I distances observed in **1** are typical for iodidobismuthates, with shorter distances for terminal (2.8577(8)-2.9190(10) Å) and longer for μ-(2.9531(8)-3.4317(11) Å) and μ_3-(3.1860(9)-3.449(1) Å) bridging iodine atoms. For example, in $(C_{13}H_{11}N_2O)_4[Bi_6I_{22}]$ [23] mean Bi-I distances range from 2.892 Å for terminal, to 3.140 Å for μ- and 3.302 Å for μ_3-bridging iodine atoms. This continues for compounds **2-4** where similar Bi-I distances can be found.

The cations in **1** display the typical features of $[(DB18C6)Na]^+$ adducts containing two trans-coordinating solvent molecules.[24] This is, again, observed similarly in compounds **2** and **3**. Crystal packing in **1** appears to be largely dominated by electrostatic interactions with the exception of a I…I interaction of 3.832 Å between I9 and I6 that links the $[Bi_6I_{22}]^{4-}$ anions into a pseudo one-dimensional strand as depicted in Figure S1 in the ESI. Such interactions with I…I distances below the sum of the van der Waals radii radii[25] have been frequently found in iodidobismuthates and are reported to have a non-negligible effect on a compound's electronic properties.[13, 18] An excerpt of the overall crystal structure is shown in Figure 1.

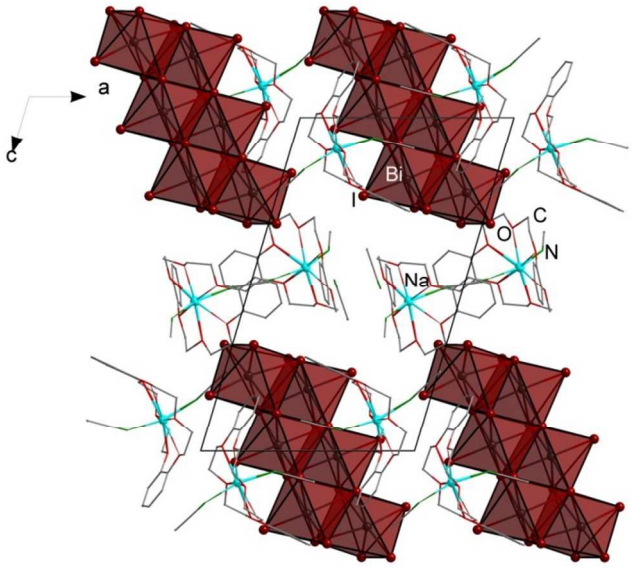

Figure 1. Excerpt of the crystal structure of **1**, viewed along the *b* axis. BiI_6 units are shown as dark red polyhedra, the crown ether molecules are represented by wire frame models. Bi atoms are shown in dark grey, I atoms in dark red, Na in light blue, O in light red, N in green and C in light grey.

The asymmetric unit of compound **2** contains one half of a $[Bi_8I_{28}]^{4-}$ anion, two $[(DB18C6)Na(MeCN)_2]^+$ cations and three MeCN solvent molecules. **2** crystallizes in the triclinic space group *P*-1. The $[Bi_8I_{28}]^{4-}$ anions, depicted in Scheme 2, represent an extension of the hexanuclear anions found in **1** by two neutral BiI_3 units and have also been reported previously for halogenidobismuthates.[13,26] A fragment of the crystal structure is shown in Figure 2. Crystal packing in **2** is surprisingly similar to that in **1**. The $[Bi_8I_{28}]^{4-}$ anions are arranged into a pseudo one-dimensional strand via an I…I interaction of 3.789 Å between I6 and I6' as depicted in Figure S2 in the ESI.

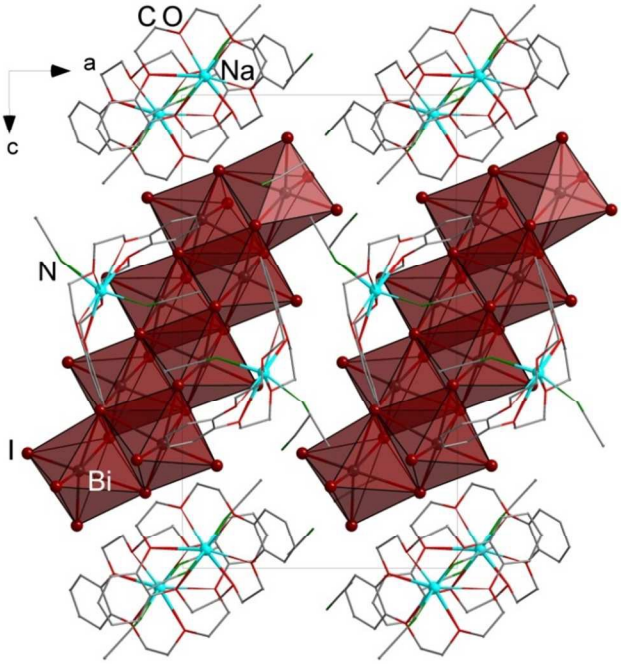

Figure 2. Fragment of the crystal structure of **2**, viewed along the *b* axis. BiI_6 units are shown as dark red polyhedra, the crown ether molecules are represented by wire frame models. Bi atoms are shown in dark grey, I atoms in dark red, Na in light blue, O in light red, N in green and C in light grey.

Compound **3** crystallizes in the triclinic space group *P*-1 a $[Bi_6I_{20}]^{2-}$ unit**,** two $[(DB18C6)Na(MeCN)_2]^+$ cations and three MeCN solvent molecules in the asymmetric unit. The iodidobismutate anions form strands running along the *a* axis, as shown in Figure 3. These strands are made up of fused $[Bi_4I_{16}]$ units, as depicted in Scheme 2. Such units can be found as molecular anions $[Bi_4I_{16}]^{4-}$,[27] but also as part of larger anions such as $[Bi_8I_{30}]^{6-}$ [28] or chains such as $^1_\infty[Bi_2I_7]^-$ or $^1_\infty[Bi_6I_{22}]^{4-}$.[13] However, condensed strands, such as those found in **3**, have not been reported previously. A related anion can be found in the chemistry of antimony. Here, several compounds with a I/Sb ratio of 3.33 have been reported.[26, 29] One of them, $[PPh_4][Sb_3I_{10}]$[26], contains a strand-like anion bearing similarity to that found in **3**. Yet, the strands differ in an important detail: In **3** the $[Bi_4I_{16}]$ units are fused in *cis*-fashion with respect to the μ_3-I atoms of the building unit, generating a twisted chain, while in $[PPh_4][Sb_3I_{10}]$ the $[Sb_4I_{16}]$ units are fused in *trans*-fashion, generating a non-twisted chain with a repeating unit of just $[Sb_3I_{10}]$ (for a direct comparison, see Figure S3 in the ESI).

An I…I interaction of 3.877 Å provides a further interconnection of the anions into a double-band as depicted in figure S4 in the ESI.

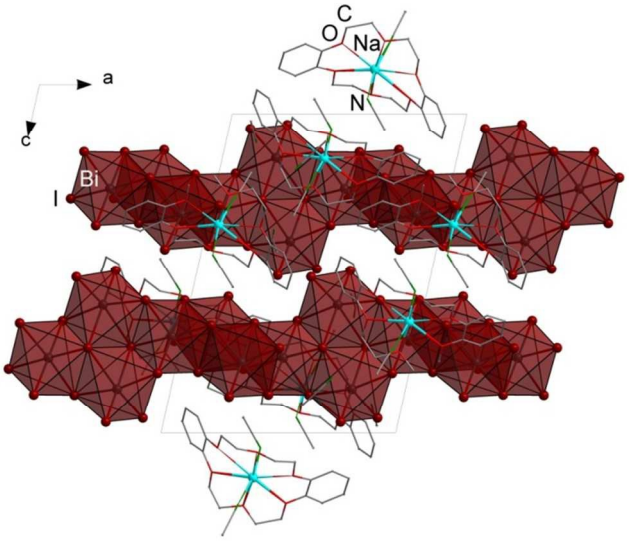

Figure 3. Excerpt of the crystal structure of **3**, viewed along the *b* axis. BiI_6 units are shown as dark red polyhedra, the crown ether molecules are represented by wire frame models. Bi atoms are shown in dark grey, I atoms in dark red, Na in light blue, O in light red, N in green and C in light grey. Fragments of two anionic $^1_\infty[Bi_6I_{20}]^{2-}$ strands are depicted.

Compound **4** crystallizes in the monoclinic space group $P2_1/n$. The asymmetric unit contains one half of a $[Bi_6I_{22}]^{4-}$ anion, two $[(DB18C6)K(MeCN)]^+$ cations and one MeCN solvent molecule. The hexanuclear anions found in **4** are very similar to those found in **1**. A fragment of the crystal structure is shown in Figure 4. In contrast to **1**, the cations in **4** form a supramolecular aggregate $[(DB18C6)K(MeCN)]_4^{4+}$ through a number of cation-π interactions[30], as depicted in Figure 5. Such interactions have been reported before in systems containing DB18C6 and alkali metal cations.[31] The supramolecular aggregate appears to provide a fitting cationic template for the hexanuclear anions, as evidenced by the facile crystallization of the compound, but also by the smaller number of solvent molecules included and the comparatively rapid rate of crystallization. Also in contrast to compounds **1**-**3**, no I…I interactions can be observed in **4**.

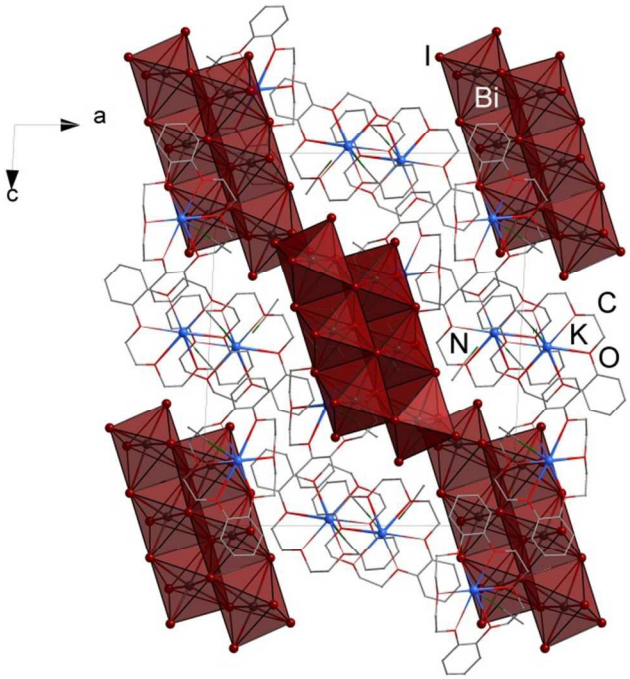

Figure 4. Fragment of the crystal structure of **4**, viewed along the *b* axis. BiI_6 units are shown as dark red polyhedra, the crown ether molecules are represented by wire frame models. Bi atoms are shown in dark grey, I atoms in dark red, K in blue, O in light red, N in green and C in light grey.

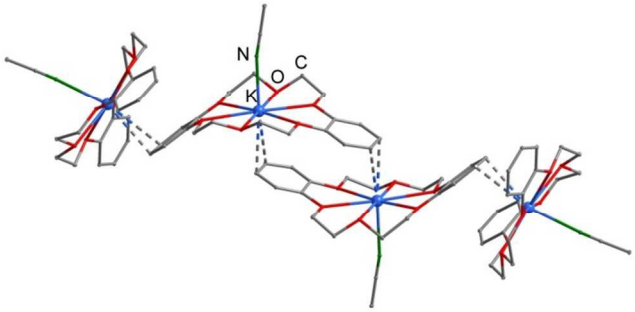

Figure 5. Supramolecular cationic aggregate $\{[(DB18C6)K(MeCN)]_4\}^{4+}$ in **4** with K-C distances in the range of 3.15-3.48 Å shown as dashed lines. K atoms are shown in blue, O in light red, N in green and C in light grey.

In essence, the $[(DB18C6)Na(MeCN)_2]^+$ units provide a roughly spherical, non-interacting cation which enforces very little structure-directing. This allows for compounds **1**-**3** to form under reagent and concentration control. This phenomenon can also be found for iodidobismuthates containing other spherical cations such as PPh_4^+ were several different compounds can be obtained depending on the reaction conditions.[13, 23, 32] In contrast to this, the supramolecular aggregate $[(DB18C6)K(MeCN)]_4^{4+}$ in **4** provides a more demanding template, allowing only the crystallization of a single species, independent of reagent ratio within a certain range.

The I/Bi ratios of the anions found in **1**-**4** and a number of literature examples are collected in table 1. The anions in **1**-**4** lie in the field of lower I/Bi ratios and represent a step-wise approach towards the binary BiI_3.

Table 1. Overview of I /Bi ratios found in iodidobismuthate anions and the parent binary.

Bi-I anion / compound	I / Bi ratio	
$[BiI_6]^{3-}$	6.00	[11]
$[Bi_2I_{10}]^{4-}$	5.00	[11]
$[Bi_2I_9]^{3-}$	4.50	[11]
$[Bi_2I_8]^{2-}$, $[Bi_3I_{12}]^{3-}$, $[Bi_4I_{16}]^{4-}$	4.00	[11]
$[Bi_5I_{19}]^{4-}$	3.80	[11]
$[Bi_8I_{30}]^{6-}$	3.75	[11]
$[Bi_6I_{22}]^{4-}$ (**1**, **4**)	3.66	This work and [11]
$[Bi_5I_{18}]^{3-}$	3.60	[11]
$[Bi_8I_{28}]^{4-}$ (**2**)	3.50	This work and [11]
$[Bi_7I_{24}]^{3-}$	3.43	[33]
$[Bi_6I_{20}]^{2-}$ (**3**)	3.33	This work
BiI_3	3.00	

Stability and thermal decomposition

Compounds **1**-**4** all display a continuous loss of solvent upon isolation from the mother liquor. Thermal investigations of freshly prepared samples can be used to estimate typical amounts of remaining solvent in **1**-**4**, summarized in the ESI. The respective thermogravimetric traces are shown in Figure 6. A complete analysis of the DTA/TG traces for each compound is provided in the ESI, Figures S9 to S12. Complete desolvation occurs between 100 and 170°C in each case, with **1** and **4** showing the greatest stability in this instance. All four compounds decompose in a single, complex step at 350°C. The extended plateau between desolvation and decomposition suggests that aside from the synthesis in solution employed here, higher temperature methods such as crown ether melts or solvothermal reactions employing non-coordinating solvents such as toluene might also be viable to produce new alkali metal crown ether based iodidobismuthates.

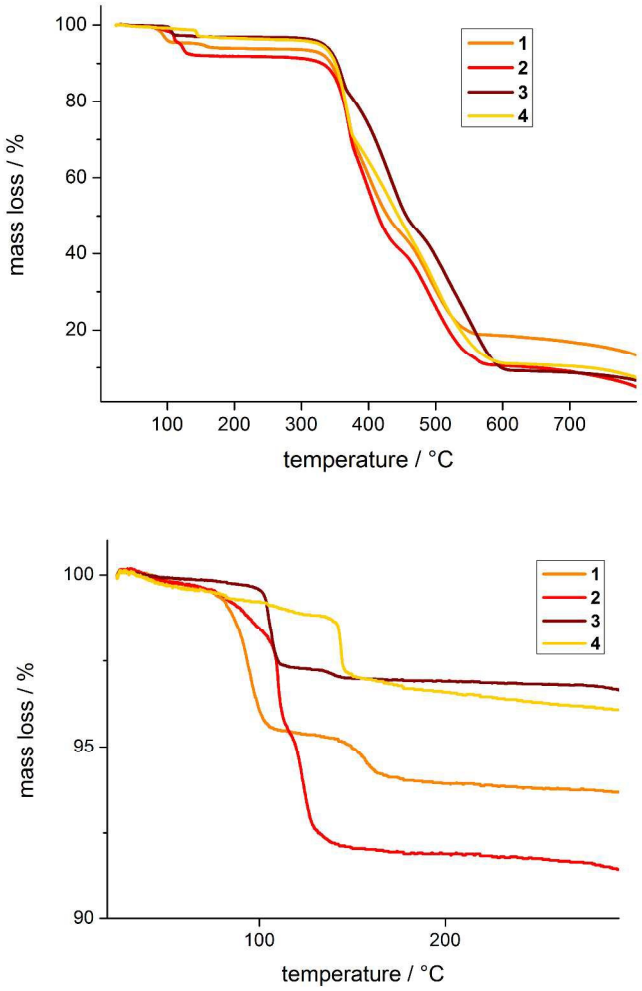

Figure 6. An overview (top) and a detailed view of the low temperature region (bottom) of the TG traces of compounds **1**-**4**.

Optical properties

UV-Vis spectra, recorded in diffuse reflection mode, are displayed in Figure 7 together with photographs of the respective crystalline material. The optical bandgaps can be estimated from the onset of absorption as 1.9 eV for **1**, **2** and **4** and as 1.8 eV for **3**. Compounds **1** and **4**, comprised of the same anionic $[Bi_6I_{22}]^{4-}$ units, show a very similar absorption behavior. Compound **2** shows a red-shift in comparison to **1** and **4**, according well with the darker crystal color and the larger $[Bi_8I_{28}]^{4-}$ units. Compound **3** displays another shift towards higher wavelength, again in accordance with darker color and the condensed, infinite building unit. The optical properties of **1**-**4** accord well with previous reports on hybrid iodidobismuthates ranging from isolated $[BiI_6]^{3-}$ octahedra[34], to dinuclear $[Bi_2I_9]^{3-}$ units[35], hexanuclear $[Bi_6I_{22}]^{4-}$ units[36] and infinite chain anions $^1_\infty[BiI_4]^-$ [13, 37] and $^1_\infty[BiI_5]^-$ [38]. These compounds are orange to dark red in color and show corresponding optical spectra. Yet, the measurements reported in the literature were each performed under slightly different conditions and in some cases using different measurement modes. This can have a non-negligible influence on the observed bandgaps, as the example of the parent binary BiI_3 illustrates: Here, researchers have reported experimental bandgap values between 2.0 and 1.7 eV, depending on compound preparation and measuring conditions.[39] Thus, conclusions based on small differences in the observed optical properties should only be drawn within one measurement series under identical conditions.

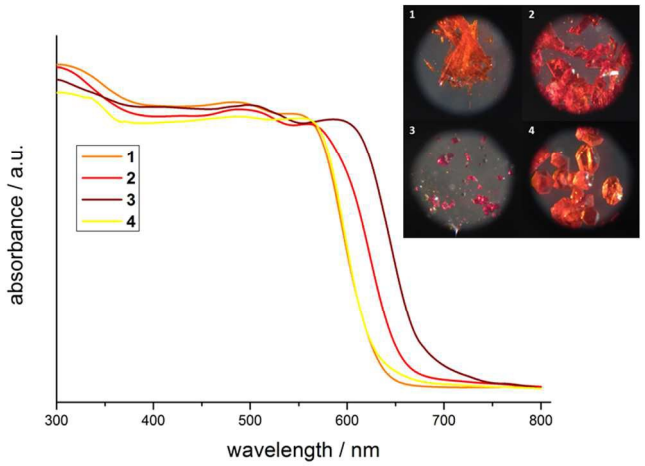

Figure 7. UV-Vis spectra of **1**-**4,** measured in diffuse reflectance mode. Photographs of the respective crystals are shown as an inset.

I…I interactions have been shown to have an influence on the optical properties of iodidometalate compounds.[13, 18] Compounds **1** and **4** both contain hexanuclear $[Bi_6I_{22}]^{4-}$ units and are fairly similar in counterion composition. I…I interactions can be observed in **1**, but not in **4**. Yet, the absorption spectra of compounds **1** and **4** display no significant difference. This stands in contrast to findings of *Mitzi* and coworkers who demonstrated that a significant shift in the excitonic bands occurs within a series of hybrid iodidobismuthates containing $^1_\infty[BiI_5]^-$ chain anions displaying different degrees of I…I interactions and resulting in different "effective" dimensionalities. Thus, it remains an open challenge for the synthesis and theoretical description of iodidometalates to determine when and how these secondary interactions will have an influence on the optical properties of a material.
The optical properties of the respective desolvated compounds have also been investigated. The UV-Vis spectra show a red-shift for all desolvated compounds with respect to their solvated counterparts (included in the ESI along with photographs of the crystalline materials before and after desolvation, Figures S21-S26). Interestingly, the red-shift upon desolvation is not uniform, but differs from compound to compound (**1**: 0.15 eV, **2**: 0.2 eV, **3**: 0.1 eV, **4**: 0.2 eV), suggesting different degrees of structural change. Unfortunately, preliminary experiments to obtain single crystals of the desolvated compounds via gentle heating under inert conditions have not been successful yet, but this interesting phenomenon will be investigated in more detail in the future.

Conclusions

In summary, the reaction of BiI_3 with DB18C6 and either NaI or KI in MeCN shows two different reaction regimes: $[(DB18C6)Na(MeCN)_2]^+$ provides a spherical cationic template, allowing for the crystallization of $[(DB18C6)Na(MeCN)_2]_4[Bi_6I_{22}]\cdot 2MeCN$ (**1**),

$[(DB18C6)Na(MeCN)_2]_4[Bi_8I_{28}]\cdot 6MeCN$ (**2**) and $[(DB18C6)Na(MeCN)_2]_2\,{}^{1}_{\infty}[Bi_6I_{20}]\cdot 3MeCN$ (**3**) under reagent control. Employing KI instead of NaI under the same reaction conditions, one obtains only a single compound with a complex supramolecular aggregate as a counter ion under template control: $[(DB18C6)K(MeCN)]_4[Bi_6I_{22}]\cdot 2MeCN$ (**4**). Compound **3** contains the first example of the ${}^{1}_{\infty}[Bi_6I_{20}]^{2-}$ iodidobismuthate anion, displaying an unprecedentedly low I/Bi ratio of 3.33. An investigation of the thermal properties of **1**-**4** shows a remarkable stability of the desolvated compounds, indicating that higher temperature reactions such as crown ether melts might be another viable route towards new iodidobismuthates. The optical properties of **1**-**4** were also investigated. **1** and **4**, with identical iodidobismuthate anions, show very similar absorption spectra, despite the additional I…I interactions present in **1** but not in **4**. Within the series **1**-**3** a continuous decrease of the optical band gap can be observed, according well with previous reports and the crystal colors.

These results show that the combination of BiI_3 with alkali metal iodides and crown ethers is a versatile reaction system capable of providing series of similar and thus well comparable compounds as well as access to previously unknown iodidobismuthate anions. Future investigations will allow access to more hybrid iodidobismuthates, thus providing us with a chance to explore the relationship of structures and optical properties more deeply, and will include the preparation of thin films from these hybrids, allowing for a comparison with the opto-electronic properties of the well-known hybrid halide perovskites.

Acknowledgements

The author gratefully acknowledges the support of Prof. Stefanie Dehnen, the Department of Chemistry and the Wissenschaftliches Zentrum für Materialwissenschaften (WZMW) of the Philipps-Universität Marburg and thanks Oliver Falkenbach of the Justus-Liebig-Universität Gießen for his help in collecting some of the PXRD patterns. Additional thanks go to Radostan Riedel for his help in obtaining a decent dataset for compound **3** and to Marvin Gernhardt and Mario Argentari for their help in obtaining additional measurements of the optical propterties and photographs of the desolvated compounds.

Notes and references

[a] Fachbereich Chemie and Wissenschaftliches Zentrum für Materialwissenschaften (WZMW), Philipps-Universität Marburg, Hans-Meerwein-Straße, 35043 Marburg, Germany. Email: johanna.heine@chemie.uni-marburg.de

Electronic Supplementary Information (ESI) available: Crystallographic details, thermal analysis, powder diffraction patterns, IR spectra, additional UV-Vis spectra. CIFs with CCDC 1050429-1050432. See DOI: 10.1039/b000000x/

1 G. C. Papavassiliou, *Prog. Solid St. Chem.*, 1997, **25**, 125-270.

2 N. Kawano, M. Koshimizu, Y. Sun, N. Yahaba, Y. Fujimoto, T. Yanagida and K. Asai, *J. Phys. Chem. C*, 2014, **118**, 9101-9106; Y. Kang, F. Wang, J. Zhang and X. Bu, *J. Am. Chem. Soc.*, 2012, **134**, 17881-17884; Y. Zhang, T. Wu, R. Liu, T. Dou, X. Bu and P. Feng, *Cryst. Growth Des.*, 2010, **10**, 2047-2049.

3 N. Leblanc, N. Mercier, L. Zorina, S. Simonov, P. Auban-Senzier and C. Pasquier, *J. Am. Chem. Soc.* 2011, **133**, 14924-14927; N. Leblanc, N. Mercier, M. Allain, O. Toma, P. Auban-Senzier and C. Pasquier, *J. Solid State Chem.* 2012, **195**, 140-148.

4 D.B. Mitzi, *J. Mater. Chem.* 2004, **14**, 2355-2365; Y. Takahashi, R. Obara, K. Nakagawa, M. Nakano, J.-y. Tokita and T. Inabe, *Chem. Mater.*, 2007, **19**, 6312-6316.

5 D. B. Mitzi, in *Functional Hybrid Materials*, ed. P. Gomez-Romero and C. Sanchez, Wiley-VCH, Weinheim, Germany, 2004, pp. 347-386.

6 I. Koutselas, P. Bampoulis, E. Maratou, T. Evagelinou, G. Pagona and G. C. Papavassiliou, *J. Phys. Chem. C*, 2011, **115**, 8475-8483.

7 C. R. Kagan, D. B. Mitzi and C. D. Dimitrakopoulos, *Science*, 1999, **286**, 945-947.

8 D. B. Mitzi, C. D. Dimitrakopoulos and L. L. Kosbar, *Chem. Mater.*, 2001, **13**, 3728-3740.

9 D. B. Mitzi, C. A. Field, W. T. Harrison and A. M. Guloy, *Nature*, 1994, **369**, 467-469.

10 M. M. Lee, J. Teuscher, T. Miyasaka, T. N. Murakami and H. J. Snaith, *Science*, 2012, **338**, 643-647; I. Chung, B. Lee, J. He, R. P. H. Chang and M. G. Kanatzidis, *Nature*, 2012, **485**, 486-489; J. Burschka,, N. Pellet, S.-J. Moon, R. Humphry-Baker, P. Gao, M. K. Nazeeruddin and M. Grätzel, *Nature*, 2013, **499**, 316-319; A. Mei, X. Li, L. Liu, Z. Ku, T. Liu, Y. Rong, M. Xu, M. Hu, J. Chen, Y. Yang, M. Grätzel and H. Han, *Science*, 2014, **345**, 295-298; B. V. Lotsch, *Angew. Chem. Int. Ed.* 2014, **53**, 635-637; H. Zhou, Q. Chen, G. Li, S. Luo, T.-b. Song, H.-S. Duan, Z. Hong, J. You, Y. Liu and Y. Yang, *Science*, 2014, **345**, 542-546.

11 L.-M. Wu, X.-T. Wu, L. Chen, *Coord. Chem. Rev.*, 2009, **253**, 2787-2804; N. Mercier, N. Louvain and W. Bi, *CrystEngComm*, 2009, **11**, 720-734; G. A. Fisher and N. C. Norman, *Advances in Inorganic Chemistry*, 1994, **41**, 233-271.

12 C. Hasselgren Arnby, S. Jagner and I. Dance, *CrystEngComm*, 2004, **6**, 257-275.

13 H. Krautscheid, *Z. anorg. allg. Chem.*, 1995, **621**, 2049-2054; D. B. Mitzi and P. Brock, *Inorg. Chem.*, 2001, **40**, 2096-2104; W. Bi and N. Mercier, *Chem. Commun.*, 2008, 5743-5745.

14 D. B. Mitzi, *Inorg. Chem.*, 2000, **39**, 6107-6113.

15 N. Yang and H. Sun, *Coord. Chem. Rev.*, 2007, **251**, 2354-2366.

16 P. C. Andrews, G. B. Deacon, C. M. Forsyth, P. C. Junk, I. Kumar and M. Maguire, *Angew. Chem. Int. Ed.*, 2006, **45**, 5638-5642; M. Schlesinger, A. Pathak, S. Richter, D. Sattler, A. Seifert, T. Rüffer, P. C. Andrews, C. A. Schalley, H. Lang and M. Mehring, *Eur. J. Inorg. Chem.*, 2014, 4218–4227; M. Mehring, *Coord. Chem. Rev.*, 2007, **251**, 974-1006.

17 L. Ye, Y. Su, X. Jin, H. Xie and C. Zhang, *Environ. Sci.: Nano*, 2014, **1**, 90-112; H. Cheng, B. Huang and Y. Dai, *Nanoscale*, 2014, **6**, 2009-2026; S. Füldner, P. Pohla, H. Bartling, S. Dankesreiter, R. Stadler, M. Gruber, A. Pfitzner and B. König, *Green Chem.*, 2011, **13**, 640-643; M.

Cherevatskaya, St. Füldner, C. Harlander, M. Neumann, S. Kümmel, St. Dankesreiter, A. Pfitzner, K. Zeitler and B. König, *Angew. Chem. Int. Ed.*, 2012, **51**, 4062-4066.

18 A. M. Goforth, M. A. Tershansy, M. D. Smith, L. Peterson Jr., J. G. Kelley, W. J. I. DeBenedetti and H.-C. zur Loye, *J. Am. Chem. Soc.*, 2011, **133**, 603-612; N. Louvain, N. Mercier and F. Boucher, *Inorg. Chem.*, 2009, **48**, 879-888; A. M. Goforth, M. D. Smith, L. Peterson Jr. and H.-C. zur Loye, *Inorg. Chem.*, 2004, **43**, 7042-7049.

19 E. Doenges, *Z. anorg. allg. Chem.*, 1950, **263**, 112-132.

20 G. M. Sheldrick, *Acta Cryst.*, 2008, **A64**, 112-122.

21 O. V. Dolomanov, L. J. Bourhis, R. J. Gildea, J. A. K. Howard and H. Puschmann, *J. Appl. Crystallogr.*, 2009, **42**, 339-341.

22 K. Brandenburg, Diamond, Crystal Impact GbR: Bonn, Germany, 2005.

23 H. Krautscheid, *Z. anorg. allg. Chem.*, 1994, **620**, 1559-1564; A. M. Goforth, J. R. Gardinier, M. D. Smith, L. Peterson Jr. and H. C. zur Loye, Inorg. *Chem. Commun.*, 2005, **8**, 684-688; I. A. Ahmed, R. Blachnik, G. Kastner and W. Brockner, *Z. anorg. allg. Chem.*, 2001, **627**, 2261-2268; B. Jaschinski, R. Blachnik and H. Reuter, *Z. anorg. allg. Chem.*, 1999, **625**, 667-672.

24 V. Shivaiah, *Inorg. Chem. Commun.*, 2006, **9**, 1191-1194.

25 R. S. Rowland and R. Taylor, *J. Phys. Chem.*, 1996, **100**, 7384-7391.

26 V. V. Sharutin, I. V. Egorova, N. N. Klepikov, E. A. Boyarkina and O. K. Sharutina, *Russ. J. Inorg. Chem.*, 2009, **54**, 1768-1778; S. Pohl, W. Saak and D. Haase, *Z. Naturforsch.* 1987, **42b**, 1493-1499.

27 Y. Chen, Z. Yang, C.-X. Guo, C.-Y. Ni, Z.-G. Ren, H.-X. Li and J.-P. Lang, *Eur. J. Inorg. Chem.*, 2010, 5326-5333.

28 C. Feldmann, *J. Solid State Chem.*, 2003, **172**, 53-58.

29 C. J. Carmalt N. C. Norman and L. J. Farrugia, *Polyhedron*, 1994, **13**, 1655-1658; S. Pohl, W. Saak, P. Mayer and A. Schmidpeter, *Angew. Chem. Int. Ed.*, 1986, **25**, 825.

30 D. A. Dougherty, *Acc. Chem. Res.*, 2013, **46**, 885-893.

31 W. Yong, J.-M. Dou, D.-Z. Zhu, Y. Liu, X. Li and P.-J. Zheng, *Acta Cryst.*, 2001, **E57**, m127-m129; B. V. Mork, A. McMillan, H. Yuen and T. D. Tilley, *Organometallics* 2004, **23**, 2855-2859.

32 S. Pohl, M. Peters, D. Haase and W. Saak, *Z. Naturforsch.*, 1994, **49b**, 741-746.

33 K. Yu. Monakhov, Ch. Gourlaouen, R. Pattacini and P. Braunstein, *Inorg. Chem.*, 2012, **51**, 1562-1568.

34 G. C. Papavassiliou, I. B. Koutselas, A. Terzis and C. P. Raptopoulou, *Z. Naturforsch.*, 1995, **50b**, 1566-1569.

35 G. C. Papavassiliou and I. B. Koutselas, *Z. Naturforsch.*, 1995, **49b**, 849-851.

36 B. Liu, L. Xu, G.-C. Guo and J.-S. Huang, *J. Solid State Chem.*, 2006, **179**, 1611-1617.

37 G. A. Mousdis, G. C. Papavassiliou, A. Terzis and C. P. Raptopoulou, *Z. Naturforsch.*, 1998, **53b**, 927-931.

38 Y. Chen, Z. Yang, X.-Y. Wu, C.-Y. Ni, Z.-G. Ren, H.-F. Wang and J.-P. Lang, *Phys. Chem. Chem. Phys.*, 2011, **13**, 5659-5667.

39 N. J. Podraza, W. Qiu, B. B. Hinojosa, H. Xu, M. A. Motyka, S. R. Phillpot, J. E. Baciak, S. Trolier-McKinstry and J. C. Nino, *J. Appl. Phys.*, 2013, **114**, 033110.

A Step Closer to the Binary: The $^{1}_{\infty}[Bi_6I_{20}]^{2-}$ Anion

Johanna Heine

A series of crown ether based iodidobismuthates explores the influence of increasing I/Bi ratio and I…I interactions on the compounds' optical properties. This includes [(Dibenzo-18-crown-6)Na(MeCN)$_2$]$_2$ $^{1}_{\infty}[Bi_6I_{20}]$, which contains a strand-like anion with an unprecedentedly low I/Bi ratio.